



Research Advances on Human-Eye-Sensitive Long Persistent Luminescence Materials

Yuhua Wang^{1,2*} and Haijie Guo^{1,2}

¹ Key Laboratory for Special Function Materials and Structure Design of the Ministry of Education, Lanzhou University, Lanzhou, China, ² Department of Materials Science, School of Physical Science and Technology, Lanzhou University, Lanzhou, China

Based on the actual application requirements of multicolor long persistent luminescence (LPL) materials, we highlight the recent developments in the last decade on human-eye-sensitive LPL materials and try to make a full list of known LPL compounds possessing wavelengths of 400–600 nm and a duration time longer than 10 h (>0.32 mcd/m²); these are more sensitive to the human eye's night vision and can be used throughout the night. We further emphasize our group research of novel LPL materials and the regulation of LPL color to enable a full palette. In the end, we try to summarize the challenges and perspectives of LPL materials for potential research directions based on our limited understandings. This review could offer new enlightenment for further exploration of new LPL materials in the visible light range and related applications.

OPEN ACCESS

Edited by:

Kenneth D. M. Harris,
Cardiff University, United Kingdom

Reviewed by:

Xiaolong Zhu,
New York University, United States
Lauren Hatcher,
Cardiff University, United Kingdom

*Correspondence:

Yuhua Wang
wyh@zu.edu.cn

Specialty section:

This article was submitted to
Solid State Chemistry,
a section of the journal
Frontiers in Chemistry

Received: 16 January 2021

Accepted: 19 March 2021

Published: 07 May 2021

Citation:

Wang Y and Guo H (2021) Research Advances on Human-Eye-Sensitive Long Persistent Luminescence Materials. *Front. Chem.* 9:654347. doi: 10.3389/fchem.2021.654347

Keywords: persistent luminescence, Eu²⁺ ions, sensitivity to human eyes, multicolor, energy transfer

INTRODUCTION

Long persistent luminescence (LPL) materials are defined as energy-saving and environmentally friendly materials that show persistent luminescence from seconds to hours after turning off the excitation sources, such as UV, visible light, X-ray, and sunlight (Zhuang et al., 2016; Li Y. et al., 2017; Xu et al., 2018; Xiong et al., 2019). Up to now, the most efficient visible light LPL materials remain blue CaAl₂O₄: Eu²⁺, Nd³⁺ and green SrAl₂O₄: Eu²⁺, Dy³⁺ (Katsumata et al., 1997, 1998; Hölsä et al., 2001), which both struggle to achieve multicolor and extensive applications. On this basis, it is the right time to provide this review to further stimulate and develop novel visible-light-emitting LPL materials and open up new applications.

As we all know, visible light can be observed and distinguished by human eyes, but the sensitivity of human eyes toward different colors is quite different. In addition, the sensitivity of the human eye also varies according to the ambient brightness (Hölsä, 2009; Poelman and Smet, 2010; Brito et al., 2012). Human eye sensitivity functions have a peak of 683 lm/W at 555 nm in photopic vision and 1,700 lm/W at 507 nm in scotopic vision (Poelman et al., 2009). That is, in scotopic vision (LPL material application conditions), human eyes are more sensitive to ~400–600 nm light. Therefore, the development of materials in this wavelength range is very important for practical applications, especially in night vision. At the same time, compared with reviews concerning LPL materials classified by emission wavelength (UV, Red, and NIR), matrices, and activators, common features, including the history, mechanism, and application of LPL materials, have been reported on repeatedly and will not be elaborated on here (Eeckhout et al., 2010, 2013; Smet et al., 2014; Zhuang et al., 2014; Li et al., 2016; Xiong and Peng, 2019; Xu and Tanabe, 2019). In this review, we mainly

focused on the following three aspects: (1) the recent development of novel LPL materials with wavelengths of 400–600 nm; (2) the approach of regulating the LPL color to achieve multicolor and discoloration on the basis of our own work; (3) the challenges and perspectives of LPL material for potential research directions. This work may be useful for the exploration of human-eye-sensitive LPL materials and the further optimization of LPL performance.

ADVANCES IN LPL MATERIALS SENSITIVE TO HUMAN EYES

As far as we know, reviews concerning the development of LPL materials with wavelengths of 400–600 nm, which play important roles in practical application, have rarely been made. In this regard, we try to make a full list of known LPL materials, possessing 400–600 nm wavelengths and a decay time longer than

TABLE 1 | Recently reported LPL materials possessing 400–600 nm wavelengths and longer than 10 h duration time (0.32 mcd/m²).

Emission peak (nm)	Materials	Activator	Co-dopant	Duration time (h)	Initial intensity (mcd/m ²)	Excitation wavelength (nm)	References
400	NaLuGeO ₄	Bi ³⁺	Eu ³⁺	~63	–	–	Wang W. et al., 2017
468	CaZnGe ₂ O ₆	Bi ³⁺	–	>12	–	254	Dou et al., 2018
473	Ba ₅ Si ₉ O ₂₁	Eu ²⁺	Dy ³⁺	>16	>100	365	Wang et al., 2015
478	BaZrSi ₃ O ₉	Eu ²⁺	Pr ³⁺	>15	238	254	Guo et al., 2017
494	Sr ₄ Al ₁₄ O ₂₅	Eu ²⁺	Dy ³⁺	>20	–	–	Luitel et al., 2013
501	Ba ₂ Zr ₂ Si ₃ O ₁₂	Eu ²⁺	Nd ³⁺	>25	155	254	Guo et al., 2019
514	BaSi ₂ O ₅	Eu ²⁺	Pr ³⁺	~38	–	254	Feng et al., 2019
523	Zn ₂ SiO ₄	Mn ²⁺	Yb ³⁺	~30	–	254	Zou et al., 2015
535	Ca ₂ MgSi ₂ O ₇	Eu ²⁺	Ce ³⁺	~20	–	Artificial daylight	Gong et al., 2009
553	Ca ₆ BaP ₄ O ₁₇	Eu ²⁺	Ho ³⁺	~47	130	254	Guo et al., 2015
560	BaSiO ₃	Eu ²⁺	Nd ³⁺ , Tm ³⁺	~10	–	Sunlight	Jia et al., 2016
567	Li ₂ SrSiO ₄	Eu ²⁺	Dy ³⁺	>15	–	254	Cheng et al., 2015
574	Sr ₃ SiO ₅	Eu ²⁺	Lu ³⁺	~20	–	365	Yu et al., 2014
580	Ca ₂ BO ₃ Cl	Eu ²⁺	Dy ³⁺	~48	>100	254	Zeng et al., 2013
580	Ca ₂ ZnSi ₂ O ₇	Eu ²⁺	Dy ³⁺	~12	–	460	Jiang et al., 2013
584	CaGa ₂ O ₄	Bi ³⁺	–	~24	–	254	Wang S. et al., 2017

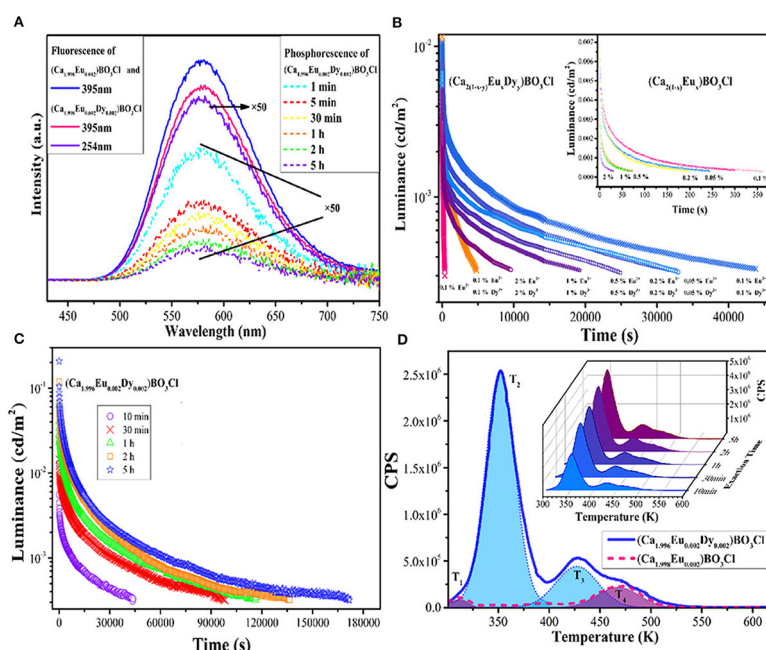
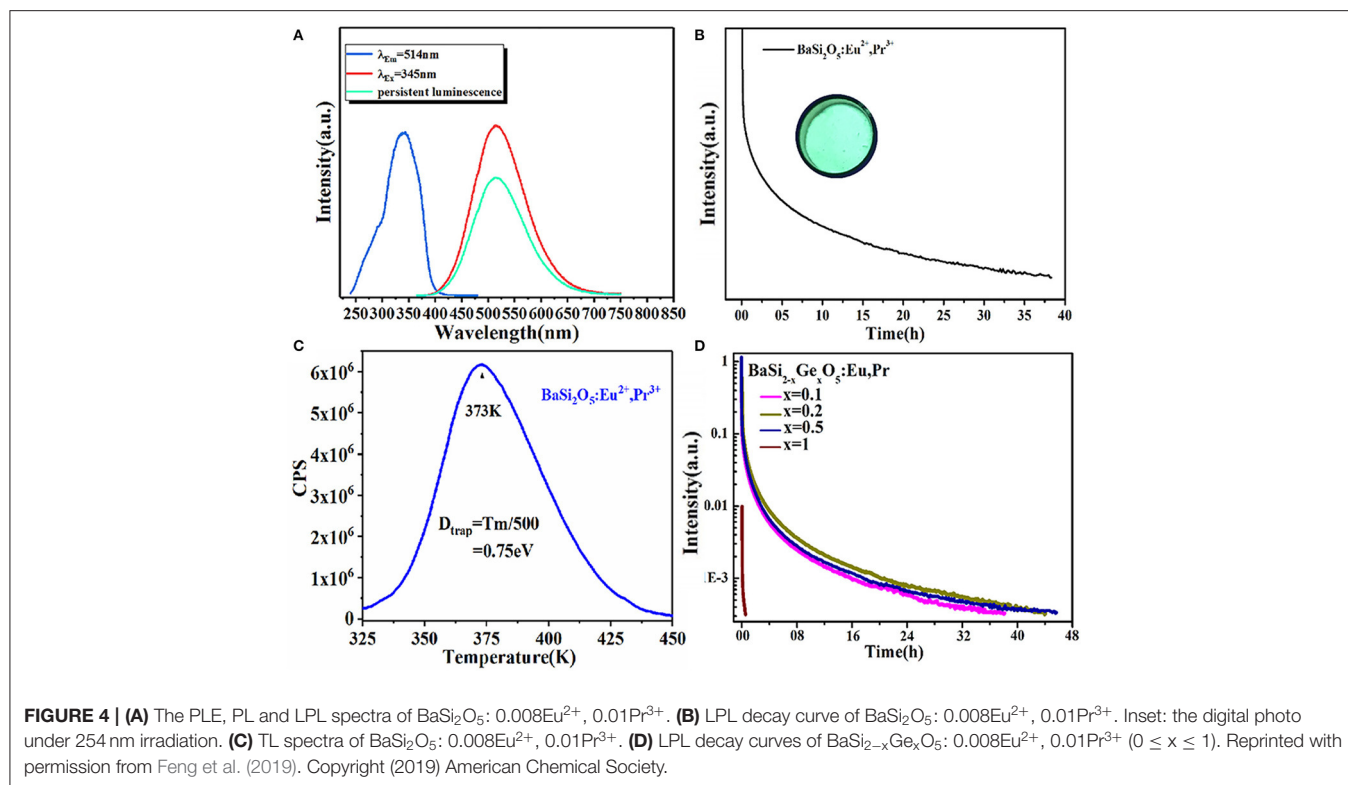


FIGURE 1 | (A) PL spectra of Ca₂BO₃Cl: 0.002Eu²⁺ and Ca₂BO₃Cl: 0.002Eu²⁺, 0.002Dy³⁺ and LPL spectra of Ca₂BO₃Cl: 0.002Eu²⁺, 0.002Dy³⁺. (B) LPL decay curves of Ca₂BO₃Cl: xEu²⁺, yDy³⁺ and Ca₂BO₃Cl: xEu²⁺ samples (inset). (C) LPL decay curves of Ca₂BO₃Cl: 0.002Eu²⁺, 0.002Dy³⁺ excited at different times. (D) TL curves of Ca₂BO₃Cl: 0.002Eu²⁺, 0.002Dy³⁺ and Ca₂BO₃Cl: 0.002Eu²⁺ excited for 10 min and TL curves of Ca₂BO₃Cl: 0.002Eu²⁺, 0.002Dy³⁺ excited for different times (inset). Reproduced by permission of The Royal Society of Chemistry.



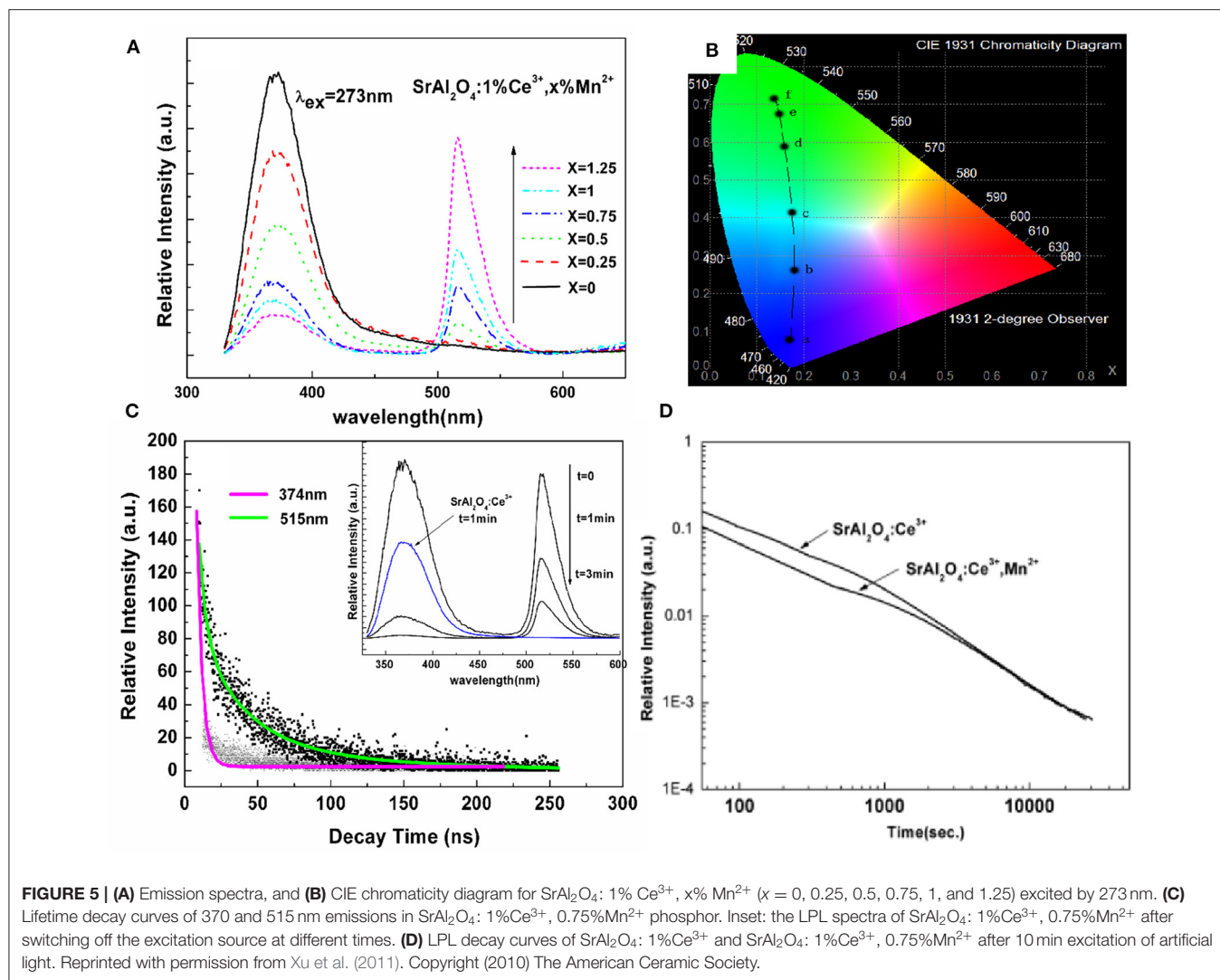
10 h ($>0.32 \text{ mcd/m}^2$), which can be used throughout the whole night, as shown in **Table 1** (Gong et al., 2009; Jiang et al., 2013; Luitel et al., 2013; Zeng et al., 2013; Yu et al., 2014; Cheng et al., 2015; Guo et al., 2015, 2017, 2019; Wang et al., 2015; Zou et al., 2015; Jia et al., 2016; Wang S. et al., 2017; Wang W. et al., 2017; Dou et al., 2018; Feng et al., 2019). Unsurprisingly, only a small amount of ions, such as Bi^{3+} and Mn^{2+} , act as activators of LPL materials. This is particularly the case for Bi^{3+} ions, which have gradually attracted people's attention in recent years. As typical examples, Wang et al. synthesized $\text{NaLuGeO}_4: \text{Bi}^{3+}, \text{Eu}^{3+}$ LPL material in 2017 (Wang W. et al., 2017). At 316 nm, a wide packet emission occurs in the 330–500 nm range, peaking at 400 nm, and this is ascribed to $^3\text{P}_{1,0} \rightarrow ^1\text{S}_0$ transitions of Bi^{3+} ions. The LPL can still be detected 63 hours after the light source is turned off. Xu et al. first realized the yellow super LPL in 2017 through Bi^{3+} ion doping in CaGa_2O_4 (Wang S. et al., 2017). Excited by 337 nm, the yellow emission, with a peak value of 584 nm, was detected. After excitation at 254 nm and 365 nm for 15 min, the LPL decay time exceeded 24 h. Bi^{3+} ions not only act as luminescence centers but also as trap centers to effectively improve electron transfer rates. In 2018, Li et al. reported that the emission range of $\text{CaZnGe}_2\text{O}_6: \text{Bi}^{3+}$ is 330–500 nm, the peak value is 468 nm, and the LPL decay time can last for more than 12 h after 254 nm light excitation for 30 min (Dou et al., 2018). Furthermore, except for Bi^{3+} ions, Mn^{2+} ions also have been recently reported to act as activators in some LPL phosphors (Lei et al., 2006; Che et al., 2008; Takahashi et al., 2011; Xu et al., 2013; Zou et al., 2015; Zhou et al., 2018). Unfortunately, the overall LPL performance is inferior. Among them, $\text{ZnSiO}_4:$

$\text{Mn}^{2+}, \text{Yb}^{3+}$, reported by Zhang et al., has a glorious green LPL performance, peaking at 523 nm (Zou et al., 2015). After 15 min of exposure to 254 nm light, the LPL duration time can last ~ 30 h (0.32 mcd/m^2). Although the past decade or so has witnessed significant advances in LPL materials with wavelengths in the range of 400–600 nm, the pattern of Eu^{2+} ions acted as activator ions and lanthanide rare-earth ions serving as trapping centers or to produce defect-related trapping center is still the most effective for most excellent LPL materials. On these grounds, we mainly introduce the research of our group on ultra LPL materials doped with Eu^{2+} ions in the next chapter.

THE APPROACH TO ACHIEVE MULTICOLOR LPL BASED ON OUR OWN WORK

Exploiting Novel LPL Materials With Rare Colors

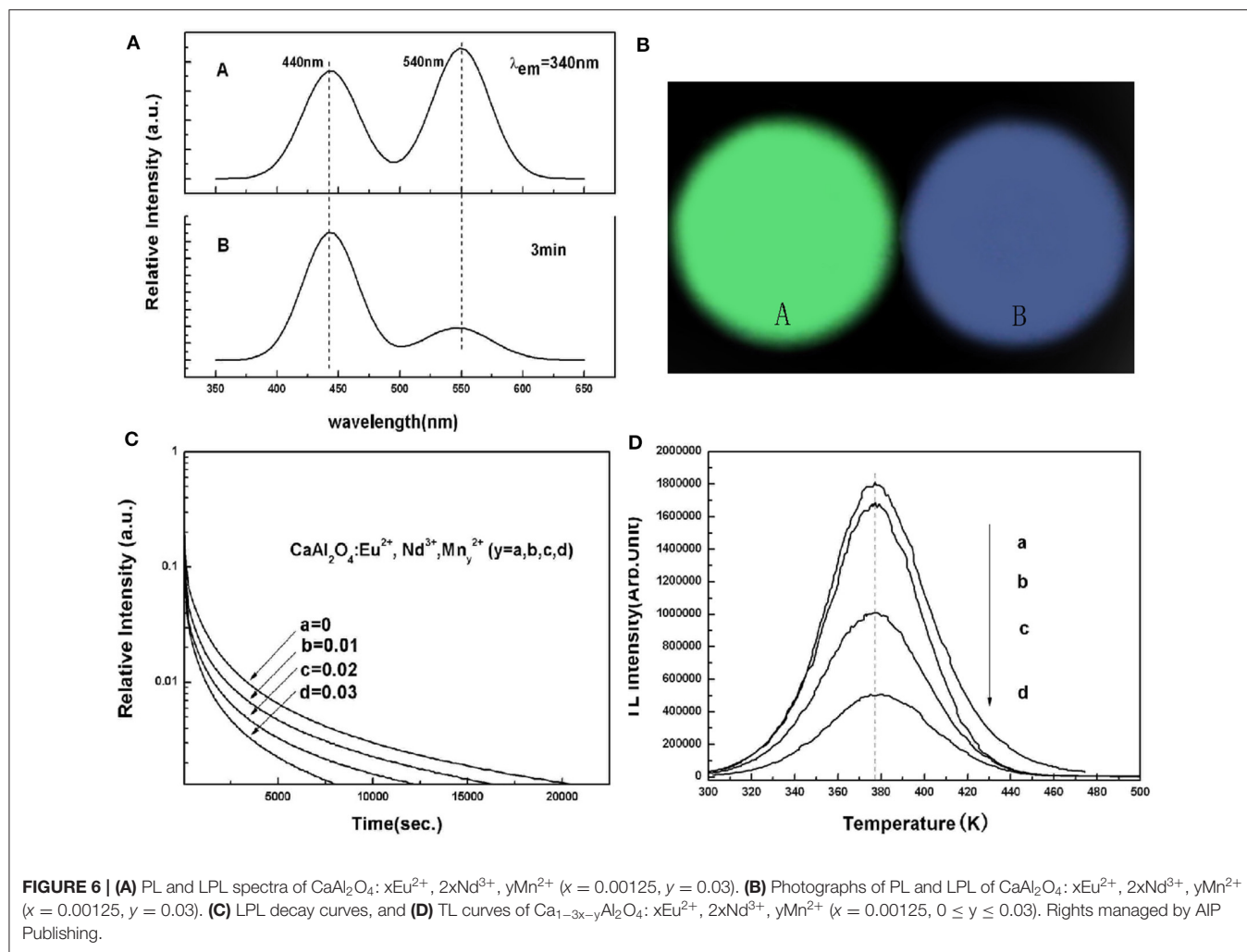
We know that yellow is often used to warn of danger or draw attention, such as yellow lights on traffic signs, large construction machinery, raincoats, etc. If the material itself continues to emit yellow light in dark conditions, this will further improve security and reliability. In addition, to date, only scattered yellow LPL materials have been reported, and the main reason is that the crystal field strength should be strong enough to reduce the 5d energy level of Eu^{2+} and thus produce yellow luminescence (Lakshminarasimhan and Varadaraju, 2008; Sun et al., 2008; Li et al., 2013, 2014). Here, we mainly present two excellent



yellow materials: $\text{Ca}_2\text{BO}_3\text{Cl}:\text{Eu}^{2+}, \text{Dy}^{3+}$ and $\text{Ca}_6\text{BaP}_4\text{O}_{17}:\text{Eu}^{2+}, \text{Ho}^{3+}$. These have been exploited by our research group (Zeng et al., 2013; Guo et al., 2015). First of all, in the $\text{Ca}_2\text{BO}_3\text{Cl}:\text{Eu}^{2+}, \text{Dy}^{3+}$ borate matrix, the photo-luminescence (PL) and LPL spectra of $\text{Ca}_2\text{BO}_3\text{Cl}:\text{Eu}^{2+}, \text{Dy}^{3+}$ have the same profile and both present an asymmetric wide emission band at 580 nm, indicating that Eu^{2+} ions occupying both Ca^{2+} lattice sites can act as a luminescent center in PL and LPL processes (Figure 1). For the representative sample of $\text{Ca}_2\text{BO}_3\text{Cl}:0.002\text{Eu}^{2+}, 0.002\text{Dy}^{3+}$, after 10 min excitation of 254 nm and 365 nm lights, the initial LPL intensity can achieve 0.01 cd/m^2 and its LPL can sustain more than 12 h above 0.32 mcd/m^2 . As the excitation time is further extended from 10 min to 5 h, the thermoluminescence (TL) intensity, LPL initial brightness, and decay time are significantly improved and prolonged. When the excitation time is up to 5 h, the charging procedure approaches saturation, and the LPL decay time reaches 48 h. This large energy storage capacity also provides benefits of optical storage and other potential applications as well (Zhuang et al., 2018).

Furthermore, as shown in Figure 2, in the $\text{Ca}_6\text{BaP}_4\text{O}_{17}$ phosphate matrix, both PL and LPL spectra of $\text{Ca}_6\text{BaP}_4\text{O}_{17}:0.02\text{Eu}^{2+}, 0.015\text{Ho}^{3+}$ only have an asymmetric broad emission band peaking at 553 nm, resulting in a bright yellow PL and LPL. Incorporation of Ho^{3+} ions can largely extend the TL characteristics and evidently elevate the LPL performance of $\text{Ca}_6\text{BaP}_4\text{O}_{17}:\text{Eu}^{2+}, \text{Ho}^{3+}$. For $\text{Ca}_6\text{BaP}_4\text{O}_{17}:0.02\text{Eu}^{2+}$, we just observe three very weak TL peaks, which indicate that the electron concentration trapped at the intrinsic defects is very low. Whereas, codoping Ho^{3+} ions makes the TL peak at 335 K greatly enhanced and largely improves the defect levels. After 15 min excitation of 254 nm and 365 nm lights, for $\text{Ca}_6\text{BaP}_4\text{O}_{17}:0.02\text{Eu}^{2+}, 0.015\text{Ho}^{3+}$, the initial LPL brightness can reach about 0.13 cd/m^2 and LPL can last more than 47 h above 0.32 mcd/m^2 .

Looking from the other side, in the dark environment ($10^{-6}\sim 10^{-2}$ cd/m^2), the maximum visual sensitivity of the human eye is 507 nm. That is to say, the human eye is most sensitive to cyan light in the dark. Because of this, our research team was striving to exploit cyan LPL materials. We first



identified $\text{Ba}_2\text{Zr}_2\text{Si}_3\text{O}_{12}: \text{Eu}^{2+}, \text{Nd}^{3+}$ cyan LPL material (Guo et al., 2019). Under 340 nm excitation, $\text{Ba}_2\text{Zr}_2\text{Si}_3\text{O}_{12}: 0.01\text{Eu}^{2+}, 0.01\text{Nd}^{3+}$ possess a broad asymmetric cyan PL band at ~ 501 nm. The LPL initial intensity is 155.5 mcd/m^2 , and the LPL duration time is near 25 h before decaying to 0.32 mcd/m^2 . On this basis, we tried to adjust the bandgap of $\text{Ba}_2\text{Zr}_2\text{Si}_3\text{O}_{12}$ by replacing Zr^{4+} with Hf^{4+} ions due to the conduction band (CB) bottom of $\text{Ba}_2\text{Zr}_2\text{Si}_3\text{O}_{12}$ is mainly composed of Zr 4d electron states, and thus the energy gap of the excited state of Eu^{2+} ions and trap center relative to CB can also be regulated. As a result, with the increase of Hf^{4+} concentration, the bottom of the CB moves upward, making the bandgap vary from 4.288 to 4.301 eV and the TL peak shift monotonically from 51 to 91°C , corresponding to the trap depth moves from 0.66 to 0.76 eV, as presented in **Figure 3**. For the optimal sample ($x = 0.5$), the initial brightness of LPL can reach 131.3 mcd/m^2 , and the LPL decay time can last for 31 h.

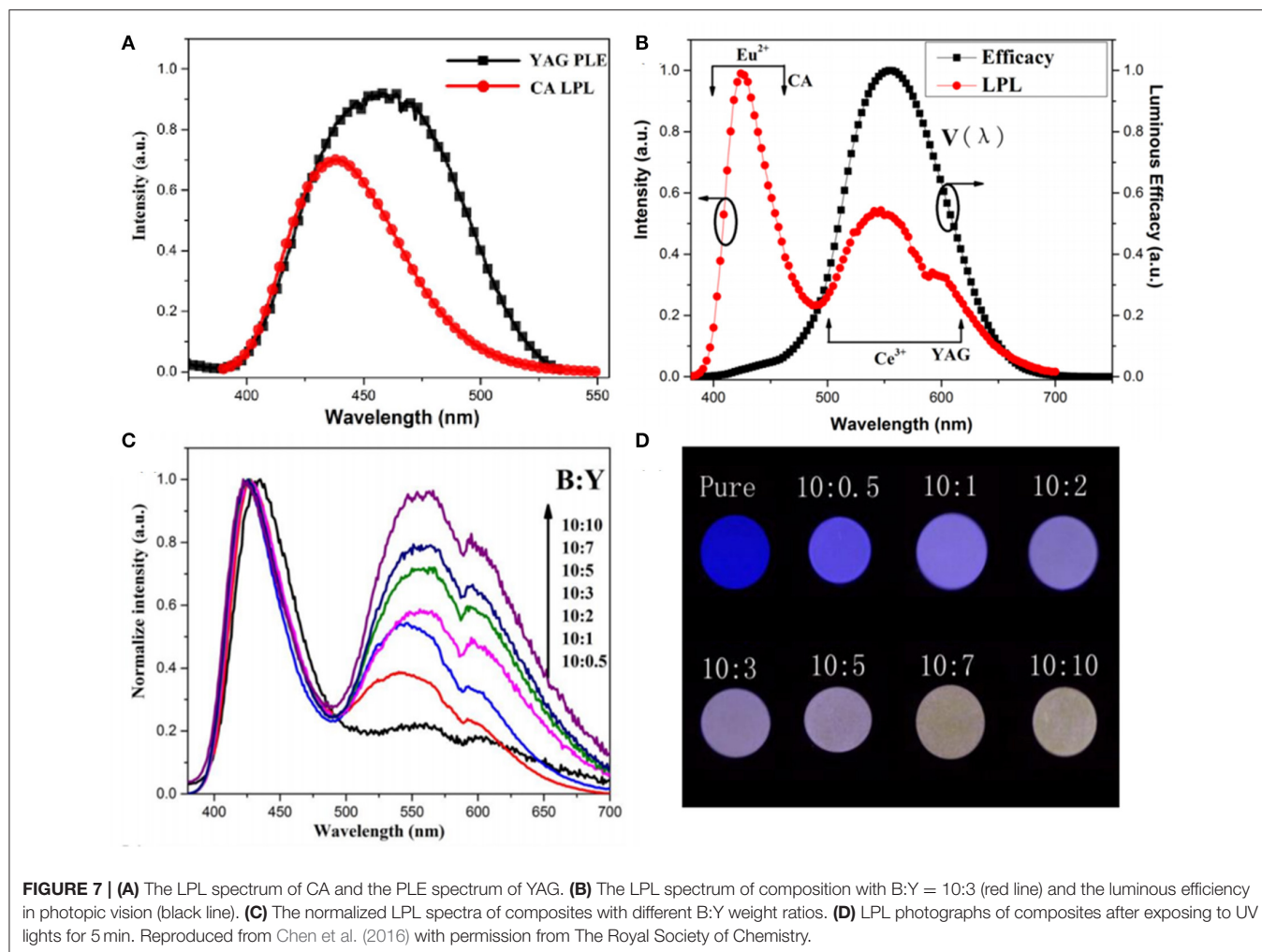
Moreover, a series of $(\text{Ba}, \text{Li}) (\text{Si}, \text{Ge}, \text{P})_2\text{O}_5: \text{Eu}^{2+}, \text{Pr}^{3+}$ cyan LPL materials were designed by adopting a solid solution strategy (Feng et al., 2019). After 10 min of excitation at 254 nm,

$\text{BaSi}_2\text{O}_5: 0.008\text{Eu}^{2+}, 0.01\text{Pr}^{3+}$ presents a strong cyan LPL located at 514 nm and the LPL duration time reaches about 38 h, which is ascribed to the increased TL intensity at 350 K by codoping Pr^{3+} ions and thus generating a number of traps suitable for LPL at room temperature (**Figure 4**). Furthermore, by means of solid solution, the LPL decay time of $(\text{Ba}, \text{Li}) (\text{Si}, \text{Ge}, \text{P})_2\text{O}_5: \text{Eu}^{2+}, \text{Pr}^{3+}$ can be prolonged from 38 to 56 h.

For the abovelisted yellow and cyan LPL materials, the LPL properties have been greatly improved. The only disadvantage, same with the current common problem of LPL materials, is that they cannot be effectively excited by sunlight. This situation limits the wide application utilizing solar energy outdoors. However, emergencies, energy conservation, and multi-color requirements can still be realized through combining with UV chip and short-term charging.

Realizing Energy Transfer

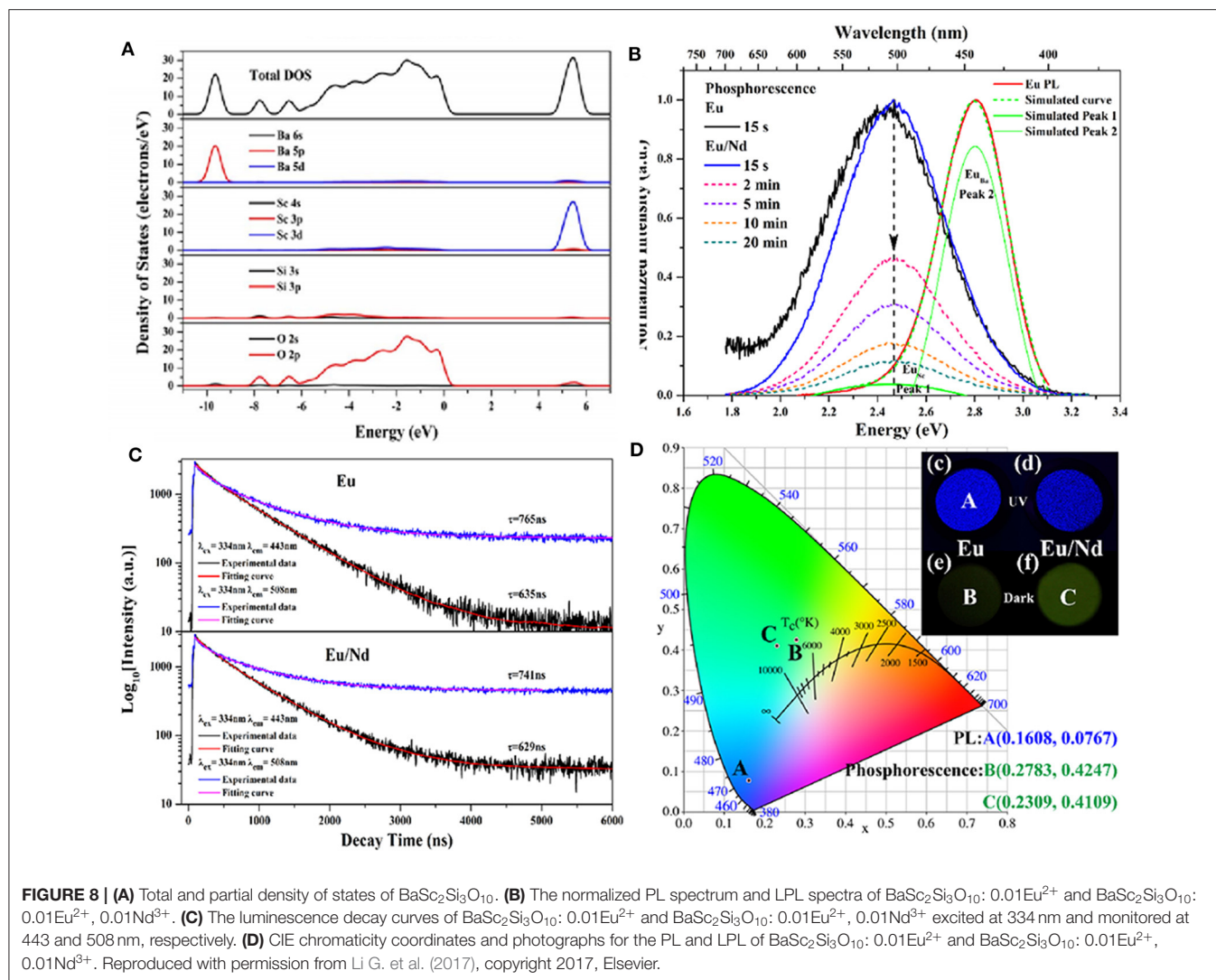
On the basis of the above work, we can easily find that it is difficult to realize the diversified LPL colors in the same material. In particular, for Eu^{2+} ions, the LPL color in most matrices is



blue-green. In a matrix, when the emission spectrum of one luminescent center overlapped with the excitation spectrum of another luminescent center, it was possible to realize non-radiative energy transfer between two luminescent centers, such as $\text{Eu}^{2+} \rightarrow \text{Mn}^{2+}$, $\text{Ce}^{3+} \rightarrow \text{Mn}^{2+}$, and $\text{Ce}^{3+} \rightarrow \text{Tb}^{3+}$ (Jia et al., 2002; Wang et al., 2003; Xu et al., 2009a, 2011; Dai, 2014). Multicolor LPL could be achieved by the energy transfer between two luminescent centers based on the existence of a large number of trap centers. As shown in Figure 5, in $\text{SrAl}_2\text{O}_4:\text{Ce}^{3+}$ blue LPL material (Xu et al., 2011), with the increase of Mn^{2+} ions concentration, the emission of Mn^{2+} ions located at 515 nm increases, and the emission band of Ce^{3+} ions at 374 nm, decreases, proving that there is an effective energy transfer from Ce^{3+} to Mn^{2+} ions. We improved the energy transfer efficiency by adjusting the concentration of Mn^{2+} ions and realized the adjustable PL color from blue light to green light. When the excitation source is removed, the energy transfer from Ce^{3+} to Mn^{2+} ions continues. However, due to the energy loss in the energy transfer process and the different decay rates of the two ions, it is difficult to ensure the uniformity of LPL color.

Among them, the inevitable energy loss in the LPL energy transfer process is also one of the main reasons for the initial LPL brightness reduction.

In addition, in $\text{CaAl}_2\text{O}_4:\text{Eu}^{2+}, \text{Nd}^{3+}$ blue LPL material, we realized the energy transfer between Eu^{2+} and Mn^{2+} ions through codoping different Mn^{2+} concentrations, and achieved the regulation of PL color from blue to green, as shown in Figure 6 (Xu et al., 2009a). Unfortunately, it can be seen from the LPL spectrum that the energy transfer efficiency of Eu^{2+} and Mn^{2+} ions is lower in the LPL decay process so that the LPL color is still blue. Even worse, the incorporation of Mn^{2+} ions leads to poor LPL performances. There are two main reasons. First, the incorporation of Mn^{2+} ions significantly reduced the concentration of the effective trap center, which can be observed from the TL spectra. Second, in the LPL decay process, the energy transfer efficiency between Eu^{2+} and Mn^{2+} ions is so low leading to inevitable energy loss. Therefore, the LPL color regulation can not be easily realized through energy transfer in the same substrate, and the LPL performance can also deteriorate.



In order to overcome the abovementioned problems of LPL color regulation through energy transfer in the same matrix, our group for the first time adopts a method of separating the trap center and luminescence center in two different matrices, utilizing the superior energy storage capacity of CaAl₂O₄: Eu²⁺, Nd³⁺ (CA), the high quantum efficiency of Y₃Al₅O₁₂: Ce³⁺ (YAG), and the great overlap of the LPL spectrum of CA and the PLE spectrum of YAG, to construct CA/YAG composites, as shown in **Figure 7** (Chen et al., 2016). The radiation energy transfer from CA to YAG achieves the LPL color adjustable characteristics from blue to white, prolongs the LPL duration time of CA/YAG composite with B:Y = 10:10–48 h compared with 19 h of CA, and heightens the initial LPL brightness to 3,200 mcd/m², which is 2.7 times higher than pure CA. The main reason for the dramatic improvement of LPL performances of CA/YAG composite is that the human visual efficiency of yellow light is much higher than that of blue light although the energy transfer efficiency reduces the overall radiation. The white LPL performances achieved by this method overcame the problem

through composite tricolor LPL materials, which required similar decay characteristics to ensure color uniformity in the LPL decay process.

Adjusting the Occupancy Rate of the Luminescent Center in Multi-Sites

In addition to the emergency lighting mentioned above, LPL materials have gradually shown more excellent performance in anti-counterfeiting and other aspects (Jiang et al., 2016; Sandhyarani et al., 2017). At present, the relatively mature fluorescent anti-counterfeiting is to realize visible light output and achieve anti-counterfeiting recognition using ultraviolet excitation. Compared with fluorescent anti-counterfeiting, the LPL anti-counterfeiting is still sustainable after turning off the excitation light source. On this basis, if the color of LPL after turning off the light source is obviously different from that of PL excited by the light source, it will greatly improve the level and force of anti-counterfeiting and provide a more effective

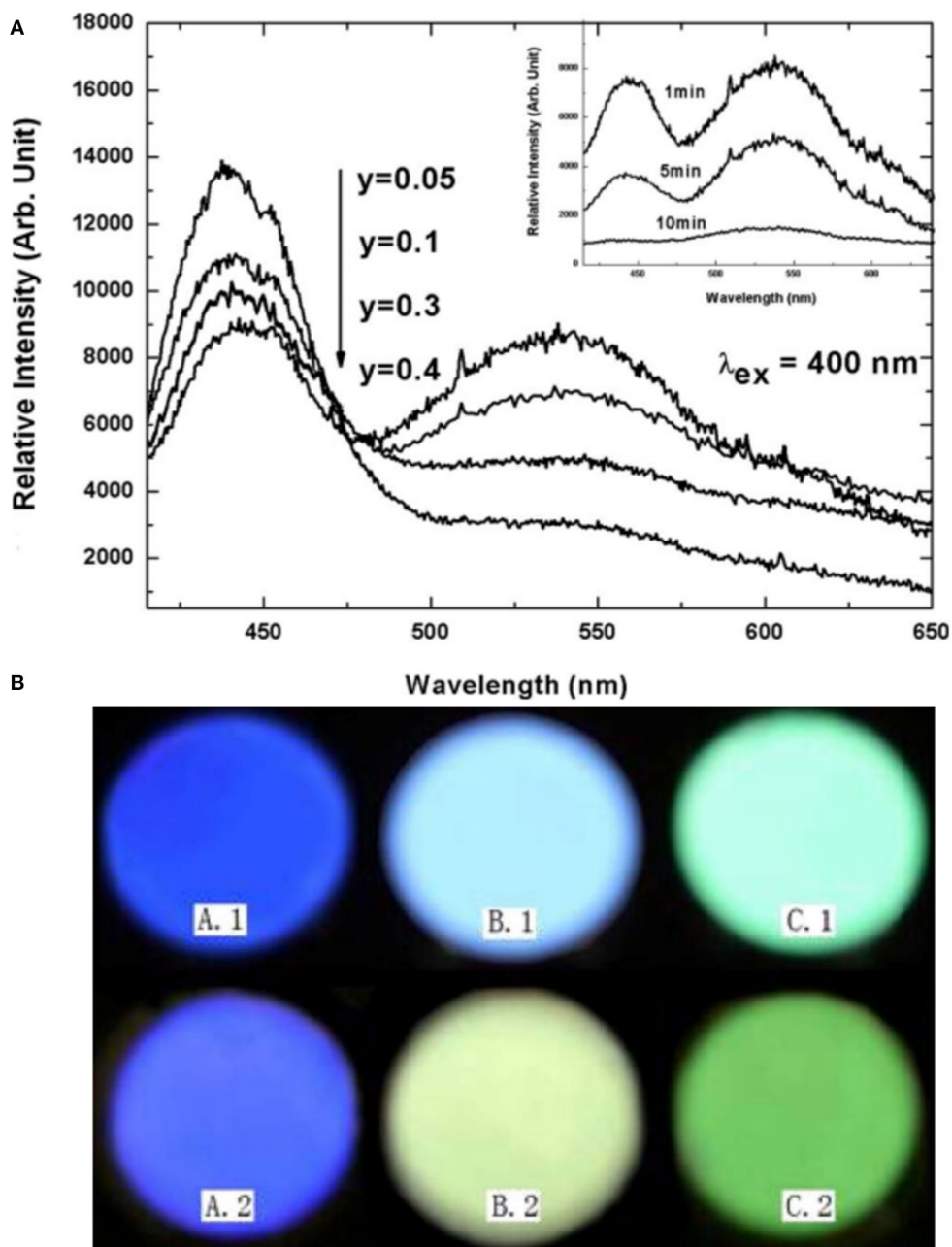


FIGURE 9 | (A) PL spectra of $\text{Ca}_{1-3x-y}\text{Al}_2\text{O}_4: x\text{Eu}^{2+}, 2x\text{Nd}^{3+}, y\text{Sr}^{2+}$ ($x = 0.00125, 0.05 \leq y \leq 0.4$), and the inset shows the LPL spectra of the sample ($y = 0.4$) measured at different times (1, 5, and 10 min). **(B)** Photos of PL (above) and LPL (below). A: $\text{CaAl}_2\text{O}_4: x\text{Eu}^{2+}, 2x\text{Nd}^{3+}$ ($x = 0.00125$); B: $\text{Ca}_{1-3x-y}\text{Al}_2\text{O}_4: x\text{Eu}^{2+}, 2x\text{Nd}^{3+}, y\text{Sr}^{2+}$ ($x = 0.00125, y = 0.4$); C: $\text{SrAl}_2\text{O}_4: x\text{Eu}^{2+}, 2x\text{Nd}^{3+}$ ($x = 0.00125$). Reproduced with permission from Xu et al. (2009b), copyright 2009, IOP Publishing.

guarantee for the safety and reliability of commodities, bills, etc. Here, we achieved this purpose mainly by regulating the Eu^{2+} ions occupation rate of multiple sites in the matrix. **Figure 8A** presents the total and partial density of states of $\text{BaSc}_2\text{Si}_3\text{O}_{10}$ calculated according to the density function theory (Li G. et al., 2017). It can be seen that the valence band (VB) is derived from 2p electronic state of O and the CB is mainly composed of 3d electronic state of Sc. **Figure 8B** displays that the PL

spectrum of $\text{BaSc}_2\text{Si}_3\text{O}_{10}: 0.01\text{Eu}^{2+}$ exhibits a wide asymmetric blue emission band peaking at 443 nm, which can be fitted well into two Gaussian peaks at 443 nm and 508 nm, ascribed to the 5d-4f transitions of Eu^{2+} ion occupying Ba and Sc sites, respectively. As shown in **Figures 8C,D**, the luminescence decay curves of $\text{BaSc}_2\text{Si}_3\text{O}_{10}: 0.01\text{Eu}^{2+}$ and $\text{BaSc}_2\text{Si}_3\text{O}_{10}: 0.01\text{Eu}^{2+}, 0.01\text{Nd}^{3+}$ prove that the green LPL at 508 nm is due to Eu^{2+} emission, not some defect level. Based on the above analysis of

the electronic structure and luminescence performances, it is believed that only Eu^{2+} ions occupying the Sc sites participate in the LPL process, while Eu^{2+} ions occupying the Ba sites are mainly involved in PL, producing an interesting phenomenon of blue PL and green LPL. Analogously, in CaAl_2O_4 : Eu^{2+} , Nd^{3+} LPL material, the green emission peak at 550 nm was enhanced while the blue emission peak at 440 nm was weakened by the partial replacement of Ca^{2+} by Sr^{2+} ions, as shown in **Figure 9** (Xu et al., 2009b). When the doping concentration of Sr^{2+} ions is 0.4 mol, the two emission peaks make the PL color appear as white light. When the excitation light source is removed, the LPL color is yellowish-green on account of the different decay characteristics of Eu^{2+} ions occupying different lattice sites.

SUMMARY AND PROSPECT

In this review, we provided the development of LPL materials with wavelengths in the 400–600 nm range, mainly introduced our group's research on developing ultra LPL materials based on Eu^{2+} ions, achieved a multicolor LPL phenomenon through

energy transfer, and realized the distinct color of PL and LPL performances through adjusting the Eu^{2+} ions occupancy rate to improve the anti-counterfeiting level. However, there are still many areas for further research and development, including but not limited to the following: (a) unearthing novel host lattices and activator ions; (b) controlling excitation and emission wavelengths; (c) structuring a unified test standard; and (d) opening up novel multifunctional application fields.

AUTHOR CONTRIBUTIONS

YW was responsible for the framework design, thinking arrangement, and text calibration of the paper. HG was responsible for the paper writing and the investigation of research progress at home and abroad. Both authors contributed to the article and approved the submitted version.

FUNDING

This work was supported by the National Natural Science Funds of China (Grant No. 51672115).

REFERENCES

- Brito, H. F., Hölsä, J., Laamanen, T., Lastusaari, M., Malkamäki, M., and Rodrigues, L. C. V. (2012). Persistent luminescence mechanisms: Human imagination at work. *Opt. Mater. Express*. 2, 371–381. doi: 10.1364/OME.2.000371
- Che, G., Li, X., Liu, C., Wang, H., Liu, Y., and Xu, Z. (2008). Long-lasting phosphorescence properties of Mn^{2+} -doped $\text{Cd}_2\text{Ge}_7\text{O}_{16}$ orange light-emitting phosphor. *Phys. Status Solidi*. 205, 194–198. doi: 10.1002/pssa.200723050
- Chen, W., Wang, Y., Zeng, W., Han, S., Li, G., Guo, H., et al. (2016). Long persistent composite phosphor CaAl_2O_4 : Eu^{2+} , $\text{Nd}^{3+}/\text{Y}_3\text{Al}_5\text{O}_{12}$: Ce^{3+} : a novel strategy to tune the colors of persistent luminescence. *N. J. Chem.* 40, 485–491. doi: 10.1002/chin.201613210
- Cheng, S., Xu, X., Han, J., Qiu, J., and Zhang, B. (2015). Design, synthesis and characterization of a novel orange-yellow long-lasting phosphor: $\text{Li}_2\text{SrSiO}_4$: Eu^{2+} , Dy^{3+} . *Powder Technol.* 276, 129–133. doi: 10.1016/j.powtec.2015.02.029
- Dai, W. (2014). Investigation of the luminescent properties of Ce^{3+} doped and $\text{Ce}^{3+}/\text{Mn}^{2+}$ co-doped $\text{CaAl}_2\text{Si}_2\text{O}_8$ phosphors. *RSC Adv.* 4, 11206–11215. doi: 10.1039/c3ra47156j
- Dou, X., Xiang, H., Wei, P., Zhang, S., Ju, G., Meng, Z., et al. (2018). A novel phosphor $\text{CaZnGe}_2\text{O}_6$: Bi^{3+} with persistent luminescence and photo-stimulated luminescence. *Mater. Res. Bull.* 105, 226–230. doi: 10.1016/j.materresbull.2018.04.047
- Eeckhout, K., Poelman, D., and Smet, P. F. (2013). Persistent luminescence in non- Eu^{2+} -doped compounds: a review. *Materials* 6, 2789–2818. doi: 10.3390/ma6072789
- Eeckhout, K., Smet, P. F., and Poelman, D. (2010). Persistent luminescence in Eu^{2+} -doped compounds: a review. *Materials* 3, 2536–2566. doi: 10.3390/ma3042536
- Feng, P., Li, G., Guo, H., Liu, D., Ye, Q., and Wang, Y. (2019). Identifying a cyan ultralong persistent phosphorescence (Ba, Li)(Si, Ge, P) $_2\text{O}_5$: Eu^{2+} , Pr^{3+} via solid solution strategy. *J. Phys. Chem. C* 123, 3102–3109. doi: 10.1021/acs.jpcc.8b11084
- Gong, Y., Wang, Y., Xu, X., Li, Y., and Jiang, Z. (2009). Enhanced long persistence of $\text{Ca}_2\text{MgSi}_2\text{O}_7$: Eu^{2+} yellow-green phosphors by co-doping with Ce^{3+} . *J. Electrochem. Soc.* 156, J295–J298. doi: 10.1149/1.3176668
- Guo, H., Chen, W., Zeng, W., Li, G., Wang, Y., Li, Y., et al. (2015). Structure and luminescence properties of a novel yellow super long-lasting phosphate phosphor $\text{Ca}_6\text{BaP}_4\text{O}_{17}$: Eu^{2+} , Ho^{3+} . *J. Mater. Chem. C* 3, 5844–5850. doi: 10.1039/c5tc00810g
- Guo, H., Wang, Y., Feng, P., Ye, Q., and Ding, S. (2019). Modifying the electronic trap distribution in $\text{Ba}_2\text{Zr}_2\text{Si}_3\text{O}_{12}$: Eu^{2+} , Nd^{3+} via regulating the composition of matrix elements. *J. Phys. Chem. C* 123, 24409–24416. doi: 10.1021/acs.jpcc.9b06775
- Guo, H., Wang, Y., Li, G., Liu, J., Feng, P., and Liu, D. (2017). Cyan emissive super-persistent luminescence and thermoluminescence in $\text{BaZrSi}_3\text{O}_9$: Eu^{2+} , Pr^{3+} phosphors. *J. Mater. Chem. C* 5, 2844–2851. doi: 10.1039/C7TC00133A
- Hölsä, J. (2009). Persistent luminescence beats the afterglow: 400 years of persistent luminescence. *Electrochem. Soc. Interface* 18, 42–45. doi: 10.1149/2.F06094IF
- Hölsä, J., Jungner, H., Lastusaari, M., and Niittykoski, J. (2001). Persistent luminescence of Eu^{2+} doped alkaline earth aluminates, MAl_2O_4 : Eu^{2+} . *J. Alloys Compd.* 323, 326–330. doi: 10.1016/S0925-8388(01)01084-2
- Jia, D., Meltzer, R., Yen, W., Jia, W., and Wang, X. (2002). Green phosphorescence of CaAl_2O_4 : Tb^{3+} , Ce^{3+} through persistence energy transfer. *Appl. Phys. Lett.* 80, 1535–1537. doi: 10.1063/1.1456955
- Jia, Y., Sun, W., Pang, R., Ma, T., Li, D., Li, H., et al. (2016). Sunlight activated new long persistent luminescence phosphor BaSiO_3 : Eu^{2+} , Nd^{3+} , Tm^{3+} : optical properties and mechanism. *Mater. Des.* 90, 218–224. doi: 10.1016/j.matdes.2015.10.130
- Jiang, K., Zhang, L., Lu, J., Xu, C., Cai, C., and Lin, H. (2016). Triple-mode emission of carbon dots: applications for advanced anti-counterfeiting. *Angew. Chem. Int. Ed.* 55, 7231–7235. doi: 10.1002/anie.201602445
- Jiang, L., Xiao, S., Yang, X., Zhang, X., Liu, X., Zhou, B., et al. (2013). Preparation and luminescence properties of yellow long-lasting phosphor $\text{Ca}_2\text{ZnSi}_2\text{O}_7$: Eu^{2+} , Dy^{3+} . *Mater. Sci. Eng. B* 178, 123–126. doi: 10.1016/j.mseb.2012.10.022
- Katsumata, T., Nabae, T., Sasajima, K., Komuro, S., and Morikawa, T. (1997). Effects of composition on the long phosphorescent SrAl_2O_4 : Eu^{2+} , Dy^{3+} phosphor crystals. *J. Electrochem. Soc.* 144, L243–L245. doi: 10.1149/1.1837931
- Katsumata, T., Nabae, T., Sasajima, K., and Matsuzawa, T. (1998). Growth and characteristics of long persistent SrAl_2O_4 - and CaAl_2O_4 -based phosphor crystals by a floating zone technique. *J. Cryst. Growth* 183, 361–365. doi: 10.1016/S0022-0248(97)00308-4
- Lakshminarasimhan, N., and Varadaraju, U. V. (2008). Luminescence and afterglow in Sr_2SiO_4 : Eu^{2+} , RE^{3+} [RE= Ce, Nd, Sm and Dy] phosphors: role of co-dopants in search for afterglow. *Mater. Res. Bull.* 43, 2946–2953. doi: 10.1016/j.materresbull.2007.12.005
- Lei, B., Li, B., Wang, X., and Li, W. (2006). Green emitting long lasting phosphorescence (LLP) properties of Mg_2SnO_4 : Mn^{2+} phosphor. *J. Luminescen.* 118, 173–178. doi: 10.1016/j.jlumin.2005.08.010

- Li, G., Wang, Y., Guo, H., Liu, J., Liu, D., and Feng, P. (2017). Electronic structure, photoluminescence and phosphorescence properties in $\text{BaSc}_2\text{Si}_3\text{O}_{10}:\text{Eu}^{2+}$, RE^{3+} ($\text{RE}^{3+} = \text{Nd}^{3+}$, Tm^{3+} , Dy^{3+} and Tb^{3+}) phosphors. *J. Luminesc.* 192, 98–104. doi: 10.1016/j.jlumin.2017.06.037
- Li, J., Lei, B., Qin, J., Liu, Y., and Liu, X. (2013). Temperature-dependent emission spectra of $\text{Ca}_2\text{Si}_5\text{N}_8:\text{Eu}^{2+}$, Tm^{3+} Phosphor and its afterglow properties. *J. Am. Ceramic Soc.* 96, 873–878. doi: 10.1111/jace.12171
- Li, Y., Gecevicius, M., and Qiu, J. (2016). Long persistent phosphors— from fundamentals to applications. *Chem. Soc. Rev.* 45, 2090–2136. doi: 10.1039/c5cs00582e
- Li, Y., Li, B., Ni, C., Yuan, S., Wang, J., Tang, Q., et al. (2014). Synthesis, persistent luminescence, and thermoluminescence properties of yellow $\text{Sr}_3\text{SiO}_5:\text{Eu}^{2+}$, RE^{3+} ($\text{RE} = \text{Ce}$, Nd , Dy , Ho , Er , Tm , Yb) and orange-red $\text{Sr}_{3-x}\text{Ba}_x\text{SiO}_5:\text{Eu}^{2+}$, Dy^{3+} phosphor. *Chem. An Asian J.* 9, 494–499. doi: 10.1002/asia.201301045
- Li, Y., Qi, S., Li, P., and Wang, Z. (2017). Research progress of Mn doped phosphors. *RSC Adv.* 7, 38318–38334. doi: 10.1039/C7RA06026B
- Luitel, H. N., Watari, T., Chand, R., Torikaki, T., Yada, M., and Mizukami, H. (2013). Tuning the luminescence color and enhancement of afterglow properties of $\text{Sr}_{(4-x-y)}\text{Ca}_x\text{Ba}_y\text{Al}_{14}\text{O}_{25}:\text{Eu}^{2+}$, Dy^{3+} phosphor by adjusting the composition. *Mater. Sci. Eng. B* 178, 834–842. doi: 10.1016/j.mseb.2013.03.014
- Poelman, D., Avci, N., and Smet, P. F. (2009). Measured luminance and visual appearance of multi-color persistent phosphors. *Opt. Express* 17, 358–364. doi: 10.1364/oe.17.000358
- Poelman, D., and Smet, P. F. (2010). Photometry in the dark: time dependent visibility of low intensity light sources. *Opt. Express* 18, 26293–26299. doi: 10.1364/OE.18.026293
- Sandhyarani, A., Kokila, M. K., Darshan, G. P., Basavaraj, R. B., Daruka Prasad, B., Sharma, S. C., et al. (2017). Versatile core-shell $\text{SiO}_2@\text{SrTiO}_3:\text{Eu}^{3+}$, Li^+ nanopowders as fluorescent label for the visualization of latent fingerprints and anti-counterfeiting applications. *Chem. Eng. J.* 327, 1135–1150. doi: 10.1016/j.cej.2017.06.093
- Smet, P. F., Botterman, J., Van den Eckhout, K., Korthout, K., and Poelman, D. (2014). Persistent luminescence in nitride and oxynitride phosphors: a review. *Optical Mater.* 36, 1913–1919. doi: 10.1016/j.optmat.2014.05.026
- Sun, X., Zhang, J., Zhang, X., Luo, Y., and Wang, X. (2008). Long lasting yellow phosphorescence and photostimulated luminescence in $\text{Sr}_3\text{SiO}_5:\text{Eu}^{2+}$ and $\text{Sr}_3\text{SiO}_5:\text{Eu}^{2+}$, Dy^{3+} phosphors. *J. Phys. D: Appl. Phys.* 41:195414. doi: 10.1088/0022-3727/41/19/195414
- Takahashi, Y., Ando, M., Ihara, R., and Fujiwara, T. (2011). Green-emissive Mn-activated nanocrystallized glass with willemite-type Zn_2GeO_4 . *Optical Mater. Express* 1, 372–378. doi: 10.1364/OME.1.000372
- Wang, P., Xu, X., Zhou, D., Yu, X., and Qiu, J. (2015). Sunlight activated long-lasting luminescence from $\text{Ba}_5\text{Si}_8\text{O}_{21}:\text{Eu}^{2+}$, Dy^{3+} phosphor. *Inorg. Chem.* 54, 1690–1697. doi: 10.1021/ic5026312
- Wang, S., Chen, W., Zhou, D., Qiu, J., Xu, X., and Yu, X. (2017). Long persistent properties of $\text{CaGa}_2\text{O}_4:\text{Bi}^{3+}$ at different ambient temperature. *J. Am. Ceramic Soc.* 100, 3514–3521. doi: 10.1111/jace.14875
- Wang, W., Sun, Z., He, X., Wei, Y., Zou, Z., Zhang, J., et al. (2017). How to design ultraviolet emitting persistent materials for potential multifunctional applications: a living example of a $\text{NaLuGeO}_4:\text{Bi}^{3+}$, Eu^{3+} phosphor. *J. Mater. Chem. C* 5, 4310–4318. doi: 10.1039/C6TC05598B
- Wang, X., Jia, D., and Yen, W. (2003). Mn^{2+} activated green, yellow, and red long persistent phosphors. *J. Lumin.* 102–103, 34–37. doi: 10.1016/S0022-2313(02)00541-0
- Xiong, P., and Peng, M. (2019). Recent advances in ultraviolet persistent phosphors. *Optical Mater.* X 2, 100022–100022. doi: 10.1016/j.omx.2019.100022
- Xiong, P., Peng, M., Cao, J., and Li, X. (2019). Near infrared mechanoluminescence from $\text{Sr}_3\text{Sn}_2\text{O}_7:\text{Nd}^{3+}$ for in situ biomechanical sensor and dynamic pressure mapping. *J. Am. Ceram. Soc.* 102, 1–11. doi: 10.1111/jace.16444
- Xu, J., Murata, D., Ueda, J., Viana, B., and Tanabe, S. (2018). Toward rechargeable persistent luminescence for the first and third biological windows via persistent energy transfer and electron trap redistribution. *Inorg. Chem.* 57, 5194–5203. doi: 10.1021/acs.inorgchem.8b00218
- Xu, J., and Tanabe, S. (2019). Persistent luminescence instead of phosphorescence: history, mechanism, and perspective. *J. Luminesc.* 205, 581–620. doi: 10.1016/j.jlumin.2018.09.047
- Xu, X., Ren, J., Chen, G., Kong, D., Gu, C., Chen, C., et al. (2013). Bright green emission from the Mn^{2+} -doped zinc gallogermanate phosphors. *Optical Mater. Express* 3, 1727–1732. doi: 10.1364/OME.3.001727
- Xu, X., Wang, Y., Li, Y., and Gong, Y. (2009a). Energy transfer between Eu^{2+} and Mn^{2+} in long-afterglow phosphor $\text{CaAl}_2\text{O}_4:\text{Eu}^{2+}$, Nd^{3+} , and Mn^{2+} . *J. Appl. Phys.* 105:083502. doi: 10.1063/1.3095514
- Xu, X., Wang, Y., Yu, X., Li, Y., and Gong, Y. (2011). Investigation of Ce-Mn energy transfer in $\text{SrAl}_2\text{O}_4:\text{Ce}^{3+}$, Mn^{2+} . *J. Am. Ceram. Soc.* 94, 160–163. doi: 10.1111/j.1551-2916.2010.04061.x
- Xu, X., Wang, Y., and Gong, Y., Li, Y. (2009b). $\text{CaAl}_2\text{O}_4:\text{Eu}^{2+}, \text{Nd}^{3+}, \text{Sr}^{2+}$: a white-light phosphor with yellow-green long afterglow. *Electrochem. Solid-State Lett.* 12, J44–J46. doi: 10.1149/1.3075902
- Yu, X., Wang, T., Xu, X., Zhou, D., and Qiu, J. (2014). Yellow photo-stimulated long persistent luminescence in strontium silicate phosphor. *ECS Solid State Lett.* 3, R4–R6. doi: 10.1149/2.006402ssl
- Zeng, W., Wang, Y., Han, S., Chen, W., Li, G., Wang, Y., et al. (2013). Design, synthesis and characterization of a novel yellow long-persistent phosphor: $\text{Ca}_2\text{BO}_3\text{Cl}:\text{Eu}^{2+}$, Dy^{3+} . *J. Mater. Chem. C*, 1, 3004–3011. doi: 10.1039/c3tc30182f
- Zhou, X., Geng, W., Guo, H., Ding, J., and Wang, Y. (2018). $\text{K}_4\text{CaGe}_3\text{O}_9:\text{Mn}^{2+}$, Yb^{3+} : a novel orange-emitting long persistent luminescent phosphor with a special nanostructure. *J. Mater. Chem. C* 6, 7353–7360. doi: 10.1039/C8TC01845F
- Zhuang, Y., Katayama, Y., Ueda, J., and Tanabe, S. (2014). A brief review on red to near-infrared persistent luminescence in transition-metal-activated phosphors. *Optical Mater.* 36, 1907–1912. doi: 10.1016/j.optmat.2014.05.035
- Zhuang, Y., Lv, Y., Li, Y., Zhou, T., Xu, J., Ueda, J., et al. (2016). Study on trap levels in $\text{SrSi}_2\text{AlO}_2\text{N}_3:\text{Eu}^{2+}, \text{Ln}^{3+}$ persistent phosphors based on host-referred binding energy scheme and thermoluminescence analysis. *Inorg. Chem.* 55, 11890–11897. doi: 10.1021/acs.inorgchem.6b01971
- Zhuang, Y., Wang, L., Lv, Y., Zhou, T., and Xie, R. (2018). Optical data storage and multicolor emission readout on flexible films using deep-trap persistent luminescence materials. *Adv. Funct. Mater.* 28:1705769. doi: 10.1002/adfm.201705769
- Zou, Z., Wu, J., Zhang, J., Ci, Z., and Wang, Y. (2015). How to induce highly efficient long-lasting phosphorescence in a lamp with a commercial phosphor: a facile method and fundamental mechanisms. *J. Mater. Chem. C* 3, 8030–8038. doi: 10.1039/c5tc01420d

Conflict of Interest: The authors declare that the research was conducted in the absence of any commercial or financial relationships that could be construed as a potential conflict of interest.

Copyright © 2021 Wang and Guo. This is an open-access article distributed under the terms of the Creative Commons Attribution License (CC BY). The use, distribution or reproduction in other forums is permitted, provided the original author(s) and the copyright owner(s) are credited and that the original publication in this journal is cited, in accordance with accepted academic practice. No use, distribution or reproduction is permitted which does not comply with these terms.